*Acta Cryst.* (1999). B**55**, 886–895

# Modulated structures of $Cs_2HgCl_4$: the 5*a* superstructure at 185 K and the 3*c* superstructure at 176 K

Bagautdin Bagautdinov,[a,b] Katrin Pilz,[a] Jens Ludecke[a] and Sander van Smaalen[a]*

[a]*Laboratory of Crystallography, University of Bayreuth, D-95440 Bayreuth, Germany, and* [b]*Institute of Solid State Physics, Russian Academy of Sciences, Chernogolovka, Moscow District, 142432 Russia.*
*E-mail: smash@uni-bayreuth.de*

(*Received 29 March 1999; accepted 10 June 1999*)

## Abstract

Crystalline dicaesium mercury tetrachloride ($Cs_2HgCl_4$) is isomorphous with $\beta$-$K_2SO_4$ (space group *Pnma*, $Z = 4$) in its normal phase at room temperature. On cooling a sequence of incommensurate and commensurate superstructures occurs, below $T$ = 221 K with modulations parallel to **a***, and below 184 K with modulations along **c***. The commensurately modulated structures at $T$ = 185 K with $\mathbf{q} = \frac{1}{5}\mathbf{a}^*$ and at $T$ = 176 K with $\mathbf{q} = \frac{1}{3}\mathbf{c}^*$ were determined using X-ray scattering with synchrotron radiation. The structure at $T$ = 185 K has superspace group $Pnma(\alpha, 0, 0)0ss$ with $\alpha = 0.2$. Lattice parameters were determined as $a = 5 \times 9.7729\,(1)$, $b = 7.5276\,(4)$ and $c = 13.3727\,(7)$ Å. Structure refinements converged to $R = 0.050$ ($R = 0.042$ for 939 main reflections and $R = 0.220$ for 307 satellites) for the section $t = 0.05$ of superspace. The fivefold supercell has space group $Pn2_1a$. The structure at $T$ = 176 K has superspace group $Pnma(0, 0, \gamma)0s0$ with $\gamma = \frac{1}{3}$. Lattice parameters were determined as $a = 9.789\,(3)$, $b = 7.541\,(3)$ and $c = 3 \times 13.418\,(4)$ Å. Structure refinements converged to $R = 0.067$ ($R = 0.048$ for 2130 main reflections, and $R = 0.135$ for 2382 satellite reflections) for the section $t = 0$. The threefold supercell has space group $P112_1/a$. It is shown that the structures of both low-temperature phases can be characterized as different superstructures of the periodic room-temperature structure. The superstructure of the 5*a*-modulated phase is analysed in terms of displacements of the Cs atoms, and rotations and distortions of $HgCl_4$ tetrahedral groups. In the 3*c*-modulated phase the distortions of the tetrahedra are relaxed, but they are replaced by translations of the tetrahedral groups in addition to rotations.

## 1. Introduction

$Cs_2HgCl_4$ belongs to the family of $A_2BX_4$ compounds. These compounds are known for their phase transitions towards incommensurate and commensurate superstructures (Cummins, 1990). For many $A_2BX_4$ compounds the sequence of phase transitions is from a periodic structure with space group *Pnma* towards an incommensurately modulated structure with $\mathbf{q} = \alpha\mathbf{a}^*$, followed by a lock-in transition. Only a few compounds exhibit a modulated state with $\mathbf{q} = \gamma\mathbf{c}^*$, all of them with either $[(CH_3)_4N]^+$ or $[(CH_3)_4P]^+$ as cation *A* (Werk *et al.*, 1990; Madariaga, Alberdi *et al.*, 1990; Madariaga, Zuniga *et al.*, 1990).

$Cs_2HgCl_4$ distinguishes itself from the other $A_2BX_4$ compounds by the fact that it has both modulated phases with $\mathbf{q} = \alpha\mathbf{a}^*$ and modulated phases with $\mathbf{q} = \gamma\mathbf{c}^*$. The study of both types of superstructures might give insight into the different ways the local strain can be resolved by the formation of superstructures.

$Cs_2HgCl_4$ exhibits a complicated sequence of phase transitions (Bagautdinov & Brown, 1997). X-ray diffraction has shown a periodic room-temperature

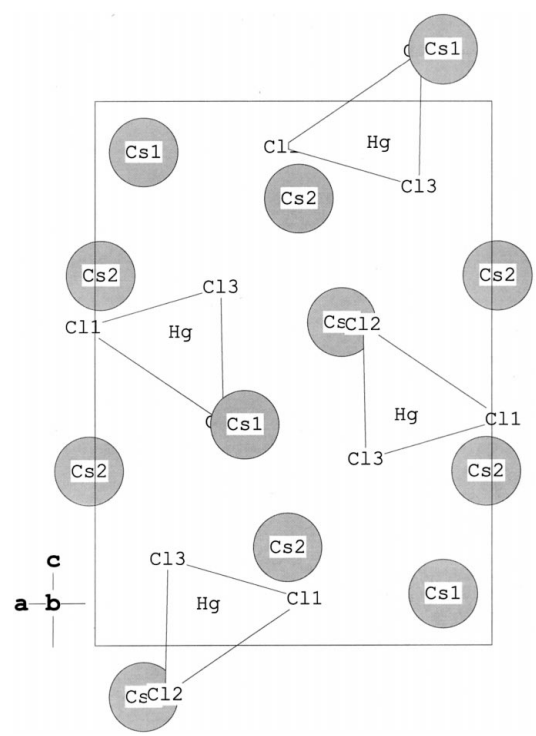


Fig. 1. Projection of the basic structure of $Cs_2HgCl_4$ along **b**. This drawing and Figs. 4 and 5 were produced with *ATOMS* (SHAPE software).

structure with orthorhombic symmetry and space group *Pnma* (Fig. 1; Linde *et al.*, 1983). On cooling transformations towards a series of superstructures were observed with the following transition temperatures and modulation wavevectors: below $T_i = 221$ K, $\mathbf{q} = (\frac{1}{5} + \delta)\mathbf{a}^*$; below $T_c = 195$ K, $\mathbf{q} = \frac{1}{5}\mathbf{a}^*$; below $T_1 = 184$ K, $\mathbf{q} = \frac{1}{3}\mathbf{c}^*$; below $T_2 = 175$ K, $\mathbf{q} = \frac{2}{5}\mathbf{c}^*$; below $T_3 = 172$ K, $\mathbf{q} = (\frac{3}{7} - \delta)\mathbf{c}^*$; below $T_4 = 169$ K, $\mathbf{q} = \frac{3}{7}\mathbf{c}^*$; below $T_5 = 163$ K, $\mathbf{q} = \frac{1}{2}\mathbf{c}^*$. The transitions have been studied by nuclear quadrupole resonance (NQR; Boguslavskii *et al.*, 1985), Raman spectroscopy and dielectric spectroscopy (Dmitriev *et al.*, 1988; Kallayev *et al.*, 1990) and X-ray diffraction (Bagautdinov & Brown, 1997).

Recently, we have studied the precursor effects above $T_i$ through the determination of the anharmonic components of the atomic displacements by the maximum entropy method (Bagautdinov *et al.*, 1998). In the present paper we give complete structural details on the 5*a* superstructure and the 3*c* superstructure, as obtained from synchrotron radiation X-ray diffraction. The results are analysed in terms of displacements of the Cs atoms and rotations, translations and distortions of the $HgCl_4$ tetrahedral anions. The modes of distortion are compared to the precursor effects above $T_i$.

## 2. Experimental

A crystal of dimensions $0.04 \times 0.08 \times 0.15$ mm$^3$ was selected for the scattering experiment. The relatively weak intensities of the superstructure reflections precluded a measurement with a rotating anode source, and synchrotron radiation was chosen instead. Synchrotron radiation X-ray diffaction was performed at beamline *F*1 of HasyLab at DESY (Hamburg, Germany), using a Siemens SMART CCD camera as detector. The specimen was cooled by a nitrogen flow cryostat. The temperature was stable to 0.5 K. Data collections were performed for the two phases at 185 and 176 K. Details of the experiment and the refinements are summarized in Table 1.†

Data reduction was performed with the standard Siemens-CCD software (*SAINT*; Siemens, 1996). The 5*a* modulated phase was indexed on a $5a \times b \times c$ superstructure. After data reduction the reflections were reindexed as main reflections and satellites using the modulation wavevector $\mathbf{q} = \frac{1}{5}\mathbf{a}^*$, according to

$$\mathbf{H} = \mathbf{h}\mathbf{a}^* + \mathbf{h}\mathbf{b}^* + \mathbf{h}\mathbf{c}^* + \mathbf{m}\mathbf{q}. \quad (1)$$

Many first-order satellites had non-zero intensities, but all second-order satellites were found to be unobserved.

† Supplementary data for this paper are available from the IUCr electronic archives (Reference: SE0279). Services for accessing these data are described at the back of the journal.

A similar procedure was followed for the 3*c* modulated structure, now with $\mathbf{q} = \frac{1}{3}\mathbf{c}^*$. For this short-period superstructure only the first-order satellites are defined, and classes of extinct satellites were not found. The structure refinements showed that the supercell symmetry of this phase is monoclinic. However, deviations from orthorhombic symmetry could not be detected in both the lattice symmetry and the Laue symmetry. The failure to find evidence for the monoclinic group in the Laue symmetry might be due to twinning of the crystal.

## 3. Symmetry and refinements

A description of the superstructures was chosen on the basis of the superspace approach (de Wolff *et al.*, 1981; van Smaalen, 1995). Superspace groups give the true symmetry of incommensurately modulated crystals, but they can also be used to analyse commensurate modulations (van Smaalen, 1987). For the present problem, the superspace approach was chosen, because it allows a unified description of the various *a*-modulated phases (Janssen, 1986) and of the various *c*-modulated phases; because both the *a*-modulated and *c*-modulated phases then are described by the same basic structure; and because the observation that all second-order satellites have zero intensities in the 5*a* superstructure implies that dependencies among the structural parameters exist, which can only be derived in the superspace approach.

The starting point for the description of the structure is the small $a \times b \times c$ unit cell, with six independent atoms in symmetry *Pnma*. The positions of the atoms in the superstructures are described as the sum of an average position $\bar{\mathbf{x}} = (\bar{x}_1, \bar{x}_2, \bar{x}_3)$, and the value of a modulation function at this point

$$x_i = \bar{x}_i + u_i(\bar{x}_{s4}) \quad (2)$$

$$\bar{x}_{s4} = t + \mathbf{q} \cdot \mathbf{x} \quad (3)$$

$$u_i(\bar{x}_{s4} + 1) = u_i(\bar{x}_{s4}) \quad (4)$$

with $i = 1, 2, 3$ representing the three space directions. $t$ is the initial phase of the modulation. $\bar{x}_{s4}$ is identified as the fourth (superspace) coordinate. Owing to the periodicity of $\mathbf{u}(\bar{\mathbf{x}}_{s4})$ (4), translation symmetry is present along this coordinate, and symmetries of the modulated structures are described by superspace groups (de Wolff *et al.*, 1981). Symmetry restrictions on the modulation functions follow from the superspace site symmetry for atoms in special positions.

Modulation functions are represented by a Fourier series

$$u_i = \sum_{n=1}^{\infty} A_{n,i} \sin(2\pi n \bar{x}_{s4}) + B_{n,i} \cos(2\pi n \bar{x}_{s4}). \quad (5)$$

Table 1. *Experimental details*

| | 3*c* Superstructure | 5*a* Superstructure |
|---|---|---|
| Crystal data | | |
| Chemical formula | $Cs_2HgCl_4$ | $Cs_2HgCl_4$ |
| Chemical formula weight | 608.2 | 608.2 |
| Temperature (K) | 176 | 185 |
| Cell setting | Orthorhombic | Orthorhombic |
| Superspace group | $Pnma(0, 0, \gamma)0s0$ | $Pnma(\alpha, 0, 0)0ss$ |
| $a$ (Å) | 9.789 (3) | 9.7729 (1) |
| $b$ (Å) | 7.541 (3) | 7.5276 (4) |
| $c$ (Å) | 13.418 (3) | 13.3727 (7) |
| Modulation wavevector | $(0, 0, \frac{1}{3})$ | $(\frac{1}{5}, 0, 0)$ |
| $Z$ | 4 | 4 |
| $t$ section ($t_0$) | 0.0 | 0.05 |
| Supercell | $a \times b \times 3c$ | $5a \times b \times c$ |
| Supercell space group | $P112_1/a$ | $Pn2_1a$ |
| $Z$ (supercell) | 12 | 20 |
| $D_x$ (Mg m$^{-3}$) | 4.078 | 4.105 |
| Radiation type | Synchrotron | Synchrotron |
| Wavelength (Å) | 0.71073 | 0.7000 |
| $\Delta f'$, $f''$ Cs | −0.368, 2.119 | −0.699, 2.068 |
| $\Delta f'$, $f''$ Hg | −2.389, 9.227 | 2.979, 9.027 |
| $\Delta f'$, $f''$ Cl | 0.148, 0.159 | 0.119, 0.154 |
| $\mu$ (mm$^{-1}$) | 23.776 | 23.52 |
| Crystal form | Bar | Bar |
| Crystal size | 0.04 × 0.08 × 0.15 | 0.04 × 0.08 × 0.15 |
| Crystal colour | Colourless | Colourless |
| Data collection | | |
| Diffractometer | Huber | Huber |
| Detector | Siemens SMART CCD camera | Siemens SMART CCD camera |
| Data collection method | Rotation images | Rotation images |
| Absorption correction | Empirical (*SADABS*; Sheldrick, 1996) | Empirical (*SADABS*; Sheldrick, 1996) |
| No. of measured reflections | 7126 | 4216 |
| No. of observed reflections | 4517 | 3033 |
| No. of independent reflections | 4512 | 1246 |
| No. of main reflections | 2130 | 939 |
| No. of satellites | 2382 | 307 |
| Criterion for observed reflections | $I > 3\sigma(I)$ | $I > 3\sigma(I)$ |
| $R_{int}$ | 0.064 | 0.087 |
| $\theta_{max}$ (°) | 30.68 | 30.68 |
| Range of $h, k, l, m$ | $-13 \rightarrow h \rightarrow 13$<br>$0 \rightarrow k \rightarrow 10$<br>$0 \rightarrow l \rightarrow 19$<br>$-1 \rightarrow m \rightarrow 1$ | $-13 \rightarrow h \rightarrow 12$<br>$-2 \rightarrow k \rightarrow 9$<br>$-16 \rightarrow l \rightarrow 8$<br>$-2 \rightarrow m \rightarrow 2$ |
| Refinement | | |
| Refinement on | $F$ | $F$ |
| $R$, $wR$ (all reflections) | 0.067, 0.101 | 0.050, 0.082 |
| $R$, $wR$ (main reflections) | 0.048, 0.074 | 0.042, 0.070 |
| $R$, $wR$ (satellites) | 0.135, 0.150 | 0.220, 0.232 |
| $S$ | 2.41 | 2.45 |
| No. of parameters | 77 | 77 |
| Weighting scheme | $[\sigma^2(F) + (0.01F)^2]^{-1}$ | $[\sigma^2(F) + (0.02F)^2]^{-1}$ |
| $(\Delta/\text{s.u.})_{max}$ | 0.002 | 0.0006 |
| $\Delta\rho_{max}$ (e Å$^{-3}$) | 0.631 | 0.685 |
| $\Delta\rho_{min}$ (e Å$^{-3}$) | −0.593 | −0.861 |
| Extinction correction | Isotropic type I (Becker & Coppens, 1974) | Isotropic type I (Becker & Coppens, 1974) |
| Extinction coefficient | 0.16 (2) | 0.07 (1) |
| Source of atomic scattering factors | *International Tables for Crystallography* (1992, Vol. C) | *International Tables for Crystallography* (1992, Vol. C) |

Generally, the Fourier amplitudes can be determined up to order $n$ if satellite reflections up to order $|m| = n$ have been observed (1) (van Aalst *et al.*, 1976).

The true symmetry of commensurately modulated structures is represented by its space group with respect to the supercell. The supercell and its symmetry can be derived from the superspace group in a unique way. It

Table 2. *Supercell space groups derived from the superspace groups for various values of* $\boldsymbol{q} = \boldsymbol{n}/\boldsymbol{m}$

The section $t$ is defined by the value of $\tau_4$ in $(i\bar{1}|000\tau_4)$.

| $n/m$ | $\tau_4 = 0$ | $\tau_4 = 1/2m (\mathrm{mod}\, 1/m)$ | Other $\tau_4$ |
|---|---|---|---|
| *Pnma*$(n/m, 0, 0)$ | | | |
| *odd/odd* | $P112/c$ | $Pn2_1a$ | $P11a$ |
| *odd/even* | $P12_1/a1$ | $Pna2_1$ | $P1a1$ |
| *even/odd* | $P2_1/n11$ | $P2_12_12_1$ | $P2_111$ |
| *Pnma*$(0, 0, n/m)$ | | | |
| *odd/odd* | $P112_1/a$ | $P2_12_12_1$ | $P112_1$ |
| *odd/even* | $P12_1/c1$ | $P2_1ca$ | $P1c1$ |
| *even/odd* | $P2_1/n11$ | $Pn2_1a$ | $Pn11$ |

appears that the supercell space group depends on the value of $t$ as well as on the values of **q**. For the superspace group *Pnma*$(\alpha, 0, 0)0ss$ the various possibilities have been derived by Janssen (1986). For the superspace group *Pnma*$(0, 0, \gamma)0s0$ they are derived here. The complete set of possibilities for both superspace groups is summarized in Table 2. The correct symmetry for the two superstructures was determined by variation of the value of $t$ in the refinements. All refinements were carried out with the system of computer programs *JANA*98 (Petricek & Dusek, 1998).

### 3.1. *The* 5*a superstructure*

From the extinction conditions the centrosymmetric superspace group *Pnma*$(\alpha, 0, 0)0ss$ was determined. Starting with the structure model for the room-temperature phase, refinement of the basic structure parameters against the main reflections resulted in a good fit with $R = 0.042$. Because only first-order satellites were observed, the refinement was continued with the first-order harmonics of the modulation functions and all data. A satisfactory fit was not obtained. This can be understood from the fact that for $\mathbf{q} = \frac{1}{5}\mathbf{a}^*$ both the first- and fourth-order harmonics contribute to the first-order satellites. Fourth-order harmonics are independent of the first-order harmonics for the atoms on special positions. For the Cl(3) atom in a general position, the first-order harmonic is sufficient to describe the complete modulation. Therefore, the fourth-order harmonics were included, and a good fit was obtained (Table 1). Introduction of the second- and third-order harmonics into the refinement did not lower the $R$-factors. Furthermore, the values for these parameters were found to be zero within their relatively large standard deviations. Therefore, they were kept at zero values for the final refinement. Second- and third-order harmonics are expected to be zero, because the second-order satellites were found with zero intensities. The final agreement factor for the satellites is rather high. This can be explained by the fact that many of the satellites are just above the level of observability. Support for this interpretation comes from the dependence of the $R$-value on the level of observability (Table 3). Furthermore, the quality of the fit was found to depend on the value of $t$. The best fit was obtained for $t = t_0 = 0.05$. This corresponds to the non-centrosymmetric space group $Pn2_1a$ for the supercell (Table 2). Coordinates, modulation amplitudes and displacement parameters are summarized in Tables 4 and 5.

Table 3. *Partial R values for the satellite reflections for the refinement of the* 5*a superstructure*

The dependency is shown of $R$ on the level of observability $I = f\sigma(I)$.

| $f$ | $R_F$ | $wR_{F^2}$ | Number of reflections |
|---|---|---|---|
| 3.0 | 21.79 | 23.14 | 307 |
| 4.0 | 16.26 | 18.26 | 172 |
| 5.0 | 13.97 | 17.03 | 111 |
| 6.0 | 12.69 | 15.81 | 84 |

### 3.2. *The* 3*c superstructure*

Analysis of the extinction conditions led to the superspace group *Pnma*$(0, 0, \gamma)0s0$. A similar procedure was followed for the refinements as it was for the 5*a* superstructure. Now, first- and second-order harmonics were required to obtain a good fit to the satellite reflections. On average, because the satellites were more intense than for the 5*a* superstructure, a better fit was obtained. The best fit was obtained for $t = t_0 = 0$, corresponding to the supercell space group $P112_1/a$ (Table 2). Since this is a monoclinic symmetry, twinning is most likely to occur. The refinements were performed with data averaged according to Laue symmetry *mmm*, thus artificially fixing the volume fractions of the domains at 0.5. Calculated structure factors were then obtained using the twinning option in *JANA*98. Coordinates, modulation amplitudes and displacement parameters are summarized in Tables 6 and 7.

## 4. Discussion

For a $N$-fold superstructure, the modulation functions are sampled at $N$ values of their arguments only. These values are found for $t = t_0 + \frac{p}{N}$ with $p = 0, \cdots, (N-1)$ (3). For $\mathbf{q} = \frac{1}{5}\mathbf{a}^*$ and $\mathbf{q} = \frac{1}{3}\mathbf{c}^*$ the consecutive $t$-values correspond to positions of atoms in consecutive unit cells. Therefore, the different atomic positions in the different unit cells are characterized by their $t$ values in Figs. 2 and 3 and in Tables 8, 9 and 10.

The distortions in $a$-modulated $A_2BX_4$ compounds have been interpreted as rotations of the $BX_4$ groups about an axis parallel to **a** and going through the $B$ atoms, combined with displacements of the $A$ cations perpendicular to the mirror planes (Fabry & Perez-Mato, 1994; Iizumi *et al.*, 1977). In accordance with this interpretation, the largest displacements of the atoms in the mirror planes are parallel to **b**, while Cl(3) has a second component of large displacement along **b** (Figs. 2 and 3). The rotations of the $HgCl_4$ groups are clearly

Table 4. *Atomic coordinates and modulation amplitudes of the 5a superstructure*

Basic structure coordinates are relative to the basic structure unit cell. Modulation amplitudes are in (Å) [equation (5)]. Standard deviations are in parentheses.

| Atom | | $x_i^0$ | $A_{1i}$ | $B_{1i}$ | $A_{4i}$ | $B_{4i}$ |
|---|---|---|---|---|---|---|
| Cs(1) | $x$ | 0.61947 (10) | 0 | 0 | −0.0147 (36) | 0.0127 (29) |
| | $y$ | 0.25 | −0.0211 (17) | 0.0580 (14) | 0 | 0 |
| | $z$ | 0.59542 (9) | 0 | 0 | −0.0013 (56) | −0.0080 (63) |
| Cs(2) | $x$ | −0.01382 (7) | 0 | 0 | −0.0137 (26) | 0.0323 (23) |
| | $y$ | 0.25 | 0.0279 (15) | −0.0512 (14) | 0 | 0 |
| | $z$ | 0.32056 (5) | 0 | 0 | −0.0094 (34) | −0.0281 (39) |
| Hg | $x$ | 0.21391 (4) | 0 | 0 | 0.0108 (17) | 0.0010 (19) |
| | $y$ | 0.25 | −0.0090 (8) | 0.0211 (9) | 0 | 0 |
| | $z$ | 0.57583 (3) | 0 | 0 | −0.0027 (24) | −0.0161 (27) |
| Cl(1) | $x$ | −0.0317 (4) | 0 | 0 | −0.0977 (18) | −0.0293 (9) |
| | $y$ | 0.25 | −0.1506 (7) | −0.0151 (6) | 0 | 0 |
| | $z$ | 0.5839 (3) | 0 | 0 | 0.0936 (13) | −0.1070 (25) |
| Cl(2) | $x$ | 0.3270 (4) | 0 | 0 | 0.0029 (70) | −0.0068 (72) |
| | $y$ | 0..25 | −0.0151 (10) | −0.2484 (12) | 0 | 0 |
| | $z$ | 0.4104 (2) | 0 | 0 | 0.1337 (13) | −0.0027 (92) |
| Cl(3) | $x$ | 0.3159 (3) | 0.0332 (60) | −0.0665 (54) | | |
| | $y$ | −0.0071 (4) | −0.0023 (41) | 0.1980 (48) | | |
| | $z$ | 0.6601 (4) | 0.0160 (81) | 0.3183 (60) | | |

Table 5. *Displacement parameters ($Å^2$) for the 5a superstructure*

| | $U^{11}$ | $U^{22}$ | $U^{33}$ | $U^{12}$ | $U^{13}$ | $U^{23}$ | $U_{iso}$ |
|---|---|---|---|---|---|---|---|
| Cs(1) | 0.0226 (5) | 0.0566 (5) | 0.1060 (8) | 0 | 0.0024 (5) | 0 | 0.0617 (4) |
| Cs(2) | 0.0221 (4) | 0.0545 (4) | 0.0263 (4) | 0 | −0.0009 (3) | 0 | 0.0343 (2) |
| Cs(1) | 0.0226 (5) | 0.0566 (5) | 0.1060 (8) | 0 | 0.0024 (5) | 0 | 0.0617 (4) |
| Cs(2) | 0.0221 (4) | 0.0545 (4) | 0.0263 (4) | 0 | −0.0009 (3) | 0 | 0.0343 (2) |
| Cl(3) | 0.051 (2) | 0.068 (2) | 0.148 (4) | −0.017 (1) | −0.037 (2) | 0.067 (2) | 0.089 (2) |

visible in the projection of one large unit cell of the 5*a* superstructure along **a** (Fig. 4). The range of orientations is estimated to encompass 9° of rotation.

A modulation along **c** is much more scarce amongst the $A_2BX_4$ compounds, and it has not been incorporated into a general model for the modulations of these compounds. Fig. 2 shows that the largest modulations are along the same directions as for the 5*a* superstructure. An obvious difference is the relatively large displacement of the Hg atoms parallel to **b**. This is found to correspond to shifts of the $HgCl_4$ groups out of the original mirror planes (Fig. 5). (The mirror planes are no longer present in the supercell space group $P2_1/a$.) Furthermore, rotations of the $HgCl_4$ groups about **a** over 9° are also found in this structure.

A more detailed analysis shows that it is not just rotations and shifts, which characterize the modulations. The four distances Hg—Cl within single $HgCl_4$ groups show a much greater variation in the 5*a* superstructure than in the 3*c* superstructure or in the room-temperature structure (Table 8). A similar behaviour is observed for the angles Cl—Hg—Cl (Table 10). The valence of mercury is the same for the three crystallographically independent atoms in the 3*c* superstructure, while definitive variations are found between the five independent Hg atoms in the 5*a* superstructure (Table 9). All these observations show that in the 5*a* superstructure the $HgCl_4$ groups are distorted as compared to their ideal geometry. The latter is present at room temperature, where the $HgCl_4$ groups are dynamically disordered, and at low temperatures.

Cs(2) is in nine coordination from Cl and it is slightly over-bonded [$V = 1.12$ at room temperature (Bagautdinov *et al.*, 1998)]. Cs(1) is in 11-coordination, but it is heavily under-bonded ($V = 0.68$). At the same time, Cs(1) is involved in the shortest Cs—Cl distance in the structure, which contributes 27% to the valence of Cs(1). [All valences are obtained with the bond-valence method (Brown, 1992) with parameters by Brese & O'Keeffe (1991).] This short distance has been made responsible for the modulations observed in $A_2BX_4$ compounds (Fabry & Perez-Mato, 1994). Surprisingly, the variations of the valences of Cs(1) and Cs(2) in both modulated structures are relatively small (Fig. 6). Still, a definite but small increase in the valence of Cs(1) is found compared with the valence of the basic structure. The largest variations are found for the valence of Cs(2) in the 5*a* superstructure. However, the average valence over the five independent Cs(2) atoms is almost equal to the valence of Cs(2) in the basic structure. In the 3*c* superstructure, the average valence of the overbonded Cs(2) is smaller than the valence in the basic structure

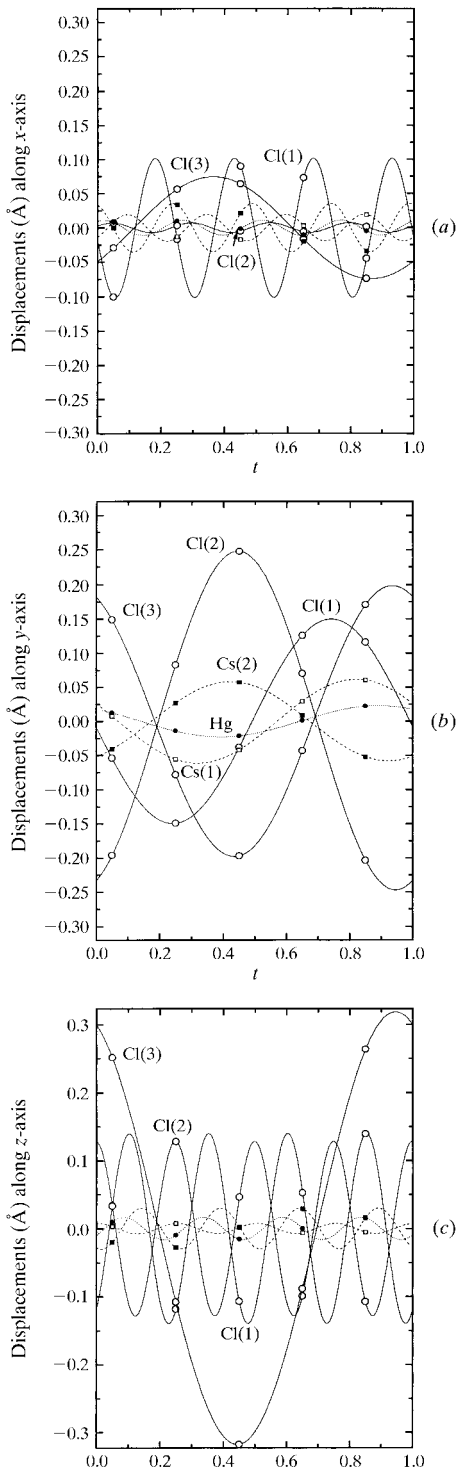


Fig. 2. The modulation functions for the 5*a* superstructure: (*a*) the *x* displacement, (*b*) the *y* displacement and (*c*) the *z* displacement. Continuous lines show the modulation functions, while symbols indicate the values that are realized for the best *t* value. Full lines and open circles pertain to the Cl atoms; dashed lines and open squares pertain to Cs(1), and filled squares represent Cs(2); dotted lines and filled circles pertain to Hg.

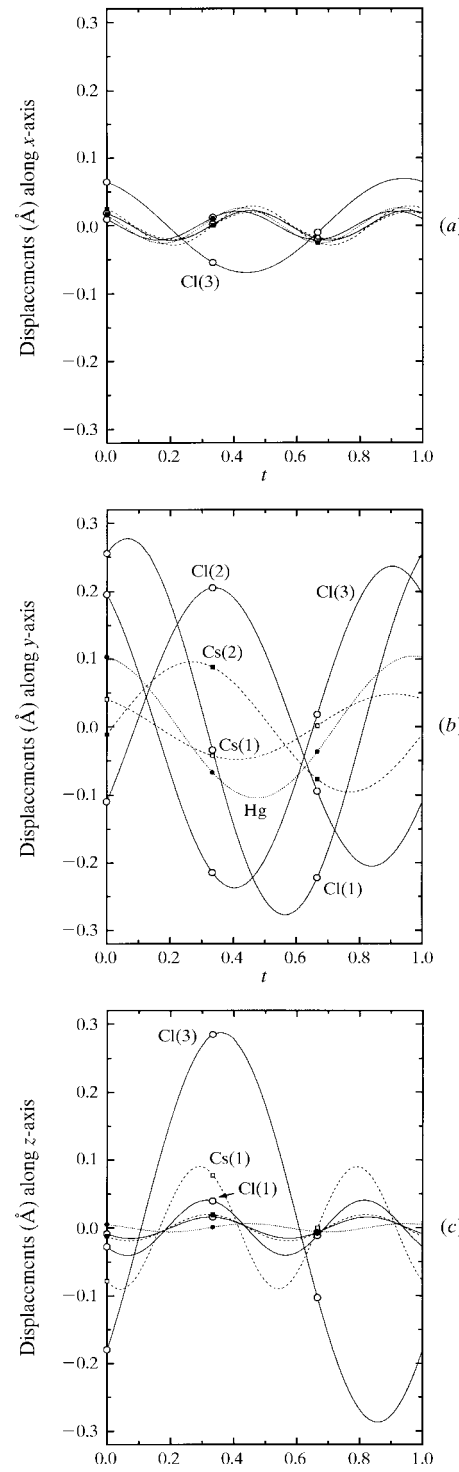


Fig. 3. The modulation functions for the 3*a* superstructure. (*a*) the *x* displacement, (*b*) the *y* displacement and (*c*) the *z* displacement. Continuous lines show the modulation functions, while symbols indicate the values that are realized for the best *t* value. Full lines and open circles pertain to the Cl atoms; dashed lines and open squares pertain to Cs(1), and filled squares represent Cs(2); dotted lines and filled circles pertain to Hg.

Table 6. *Atomic coordinates and modulation amplitudes of the 3c superstructure*

Basic structure coordinates are relative to the basic structure unit cell. Modulation amplitudes are in (Å) [equation (5)]. Standard deviations are in parentheses.

| Atom | | $x_i^0$ | $A_{1i}$ | $B_{1i}$ | $A_{2i}$ | $B_{2i}$ |
|---|---|---|---|---|---|---|
| Cs(1) | $x$ | 0.61963 (6) | 0 | 0 | 0.0185 (9) | −0.0076 (11) |
| | $y$ | 0.25 | 0.0305 (6) | 0.0371 (6) | 0 | 0 |
| | $z$ | 0.59598 (6) | 0 | 0 | −0.0114 (14) | 0.0893 (12) |
| Cs(2) | $x$ | −0.01369 (4) | 0 | 0 | 0.0208 (8) | 0.0198 (10) |
| | $y$ | 0.25 | 0.0678 (5) | −0.0678 (5) | 0 | 0 |
| | $z$ | 0.32034 (3) | 0 | 0 | −0.0154 (9) | 0.0117 (8) |
| Hg | $x$ | 0.21371 (3) | 0 | 0 | 0.0258 (5) | 0.0024 (6) |
| | $y$ | 0.25 | 0.0899 (3) | 0.0531 (3) | 0 | 0 |
| | $z$ | 0.57575 (2) | 0 | 0 | 0.0060 (5) | −0.0011 (5) |
| Cl(1) | $x$ | −0.0320 (3) | 0 | 0 | 0.021 (3) | 0.005 (4) |
| | $y$ | 0.25 | 0.2770 (42) | −0.0154 (36) | 0 | 0 |
| | $z$ | 0.5839 (2) | 0 | 0 | 0.005 (5) | 0.040 (4) |
| Cl(2) | $x$ | 0.3257 (2) | 0 | 0 | 0.020 (3) | 0.010 (4) |
| | $y$ | 0.25 | 0.0300 (29) | −0.2031 (32) | 0 | 0 |
| | $z$ | 0.4109 (1) | 0 | 0 | −0.007 (4) | 0.014 (3) |
| Cl(3) | $x$ | 0.3159 (2) | 0.0585 (22) | 0.0371 (23) | | |
| | $y$ | 0.5062 (2) | 0.1670 (22) | 0.1686 (21) | | |
| | $z$ | 0.6609 (4) | −0.1351 (32) | −0.2536 (30) | | |

Table 7. *Displacement parameters ($Å^2$) for the 3c superstructure*

| Atom | $U^{11}$ | $U^{22}$ | $U^{33}$ | $U^{12}$ | $U^{13}$ | $U^{23}$ | $U_{iso}$ |
|---|---|---|---|---|---|---|---|
| Cs(1) | 0.0253 (3) | 0.0584 (3) | 0.1126 (6) | 0 | 0.0008 (3) | 0 | 0.0654 (2) |
| Cs(2) | 0.0263 (2) | 0.0546 (3) | 0.0308 (2) | 0 | −0.0009 (1) | 0 | 0.0373 (1) |
| Hg | 0.0286 (2) | 0.0417 (2) | 0.0322 (2) | 0 | 0.00113 (9) | 0 | 0.0342 (1) |
| Cl(1) | 0.022 (1) | 0.162 (2) | 0.064 (2) | 0 | 0.0057 (9) | 0 | 0.083 (1) |
| Cl(2) | 0.032 (1) | 0.125 (2) | 0.0315 (8) | 0 | 0.0075 (8) | 0 | 0.0629 (8) |
| Cl(3) | 0.0494 (9) | 0.080 (1) | 0.156 (2) | 0.0170 (8) | −0.035 (2) | −0.072 (1) | 0.0950 (8) |

Table 8. *Bond lengths (Å) for the room-temperature structure and the 5a and 3c superstructures*

| | *Pnma* | 5*a* superstructure | | | | | 3*c* superstructure | | |
|---|---|---|---|---|---|---|---|---|---|
| $t$ | – | 0.05 | 0.25 | 0.45 | 0.65 | 0.85 | 0.0 | 0.333 | 0.667 |
| Hg—Cl(1) | 2.399 | 2.512 | 2.431 | 2.309 | 2.325 | 2.452 | 2.420 | 2.408 | 2.417 |
| Hg—Cl(2) | 2.471 | 2.461 | 2.350 | 2.431 | 2.566 | 2.597 | 2.489 | 2.473 | 2.477 |
| Hg—Cl(3) | 2.456 | 2.456 | 2.479 | 2.503 | 2.445 | 2.435 | 2.476 | 2.465 | 2.463 |
| Hg—Cl(3)′ | 2.456 | 2.465 | 2.432 | 2.471 | 2.470 | 2.494 | 2.441 | 2.481 | 2.483 |
| Average | 2.446 | 2.474 | 2.423 | 2.429 | 2.452 | 2.495 | 2.457 | 2.457 | 2.460 |
| Max–min | 0.072 | 0.056 | 0.129 | 0.194 | 0.241 | 0.162 | 0.069 | 0.073 | 0.066 |

(Fig. 6). This is again an indication that the modulation in this phase is accompanied with a large amount of internal strain.

The directions of largest modulations of all atoms correlate with the largest components of the displacement tensors found for the refinement of the structure at room temperature (Bagautdinov *et al.*, 1998). However, the anisotropy of the displacement tensors is not reduced in the modulated phases (Tables 6 and 7). The general reduction in sizes is compatible with the lower temperatures of the modulated structures. The largest anharmonic contributions to the displacement factors at room temperature have been found for Cs(1), Cl(1) and Cl(3) (Bagautdinov *et al.*, 1998). In accordance with the observed modulation amplitudes at lower temperatures, the anharmonicity of Cl(1) involves displacements perpendicular to the mirror planes. The major anharmonic terms for Cl(3) involve displacements parallel to **c**, and the largest modulation is found for this atom along this direction. However, the modulation of Cl(2) does not have a counterpart in anharmonic terms in its displacement tensor at room temperature, and Cs(1) has an anharmonic displacement parallel to **c**, while its largest displacement is along **b**. The conclusion must be that the directions of the modulations at low temperatures are not directly correlated with the anharmonicity of the displacement factors at room temperature.

## 5. Conclusions

The structures of $Cs_2HgCl_4$ have been determined for the 5*a* superstructure at $T$ = 185 K and for the 3*c*

Table 9. *Bond valences between Hg and Cl and the valence of Hg for the room-temperature structure and the 5a and 3c superstructures*

| | *Pnma* | 5*a* superstructure | | | | | 3*c* superstructure | | |
|---|---|---|---|---|---|---|---|---|---|
| *t* | – | 0.05 | 0.25 | 0.45 | 0.65 | 0.85 | 0.0 | 0.333 | 0.667 |
| Hg—Cl(1) | 0.671 | 0.494 | 0.615 | 0.856 | 0.819 | 0.581 | 0.634 | 0.655 | 0.639 |
| Hg—Cl(2) | 0.552 | 0.567 | 0.766 | 0.615 | 0.427 | 0.393 | 0.526 | 0.549 | 0.543 |
| Hg—Cl(3) | 0.575 | 0.575 | 0.540 | 0.506 | 0.592 | 0.609 | 0.545 | 0.561 | 0.564 |
| Hg—Cl(3)′ | 0.575 | 0.561 | 0.614 | 0.552 | 0.554 | 0.519 | 0.599 | 0.537 | 0.535 |
| Valence (Hg) | 2.373 | 2.197 | 2.535 | 2.529 | 2.392 | 2.102 | 2.304 | 2.302 | 2.281 |

Table 10. *Bond angles (°) in the $HgCl_4$ groups for the room-temperature structure and the 5a and 3c superstructures*

| | *Pnma* | 5*a* superstructure | | | | | 3*c* superstructure | | |
|---|---|---|---|---|---|---|---|---|---|
| *t* | – | 0.05 | 0.25 | 0.45 | 0.65 | 0.85 | 0.0 | 0.333 | 0.667 |
| Cl(1)—Hg—Cl(2) | 118.2 | 119.5 | 118.0 | 117.4 | 119.5 | 120.9 | 118.7 | 119.0 | 118.6 |
| Cl(1)—Hg—Cl(3) | 112.7 | 110.0 | 112.1 | 114.6 | 114.7 | 110.7 | 111.0 | 109.8 | 117.0 |
| Cl(1)—Hg—Cl(3)′ | 112.7 | 114.6 | 115.1 | 112.3 | 109.8 | 111.4 | 113.7 | 114.5 | 109.8 |
| Cl(2)—Hg—Cl(3) | 103.3 | 105.0 | 101.7 | 101.1 | 103.3 | 106.3 | 103.1 | 105.6 | 102.4 |
| Cl(2)—Hg—Cl(3)′ | 103.3 | 101.4 | 104.0 | 105.9 | 104.1 | 101.2 | 104.6 | 102.4 | 104.2 |
| Cl(3)—Hg—Cl(3)′ | 105.5 | 105.0 | 104.3 | 104.2 | 104.1 | 104.9 | 104.3 | 104.3 | 103.0 |
| Max–min | 14.9 | 18.1 | 16.2 | 16.3 | 16.2 | 19.8 | 15.6 | 16.6 | 16.1 |

superstructure at $T = 176$ K. It is **a**-modulation that is the usual type of superstructure ordering in $A_2BX_4$ compounds. Assuming the superstructures to represent a distortion according to the $\Sigma_2$ normal mode of *Pnma*, it has been proposed that the modulations involve rotations of the $BX_4$ groups about axes in the mirror planes together with displacements of the $A$ cations perpendicular to the mirror planes (Fabry & Perez-Mato, 1994). Here we have shown that atomic displacements in the 5*a* superstructure involve the $\Sigma_2$ mode, but that in addition distortions of the $HgCl_4$ groups occur. The 3*c* superstructure is found to contain undistorted $HgCl_4$ groups. In addition to rotations of similar sizes as in the 5*a* superstructure, the modulation of the $HgCl_4$ groups now involves shifts away from the mirror plane of the parent phase. Apparently, the distortions of $HgCl_4$ groups are responsible for internal strain, which make **a**-modulated structures energetically less favourable than **c**-modulated structures.

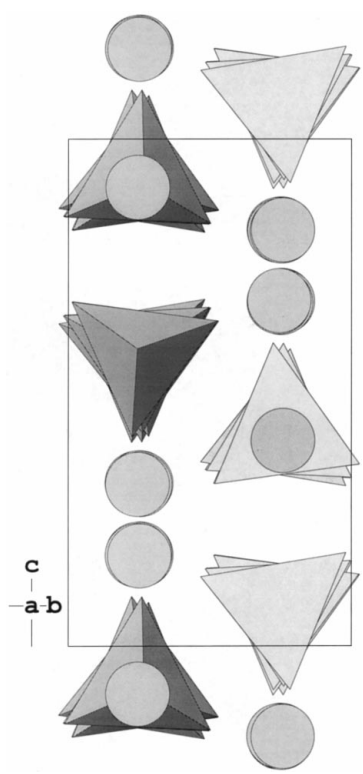


Fig. 4. Projection of one supercell of the 5*a* superstructure along **a**. $HgCl_4$ groups are represented by tetrahedra. Note that in this projection the orientations (rotations) are almost the same for the first and the fifth tetrahedra, and for the second and the third tetrahedra in one supercell along **a**.

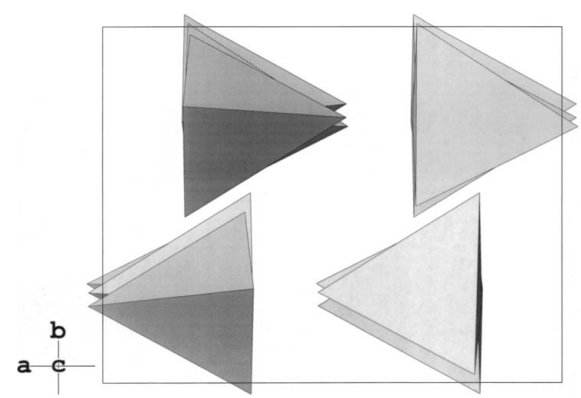


Fig. 5. Projection of one supercell of the 3*c* superstructure along **c**. $HgCl_4$ groups are represented by tetrahedra. The shifts of these groups are clearly visible. The Cs atoms are not shown.

Both superstructures are described by centrosymmetric superspace groups based on the same space group for the average structure (Table 1). The latter property stresses that both superstructures are generated through different distortions of the same basic structure. The superspace description thus provides a unified description of the symmetries of the two kinds of modulations.

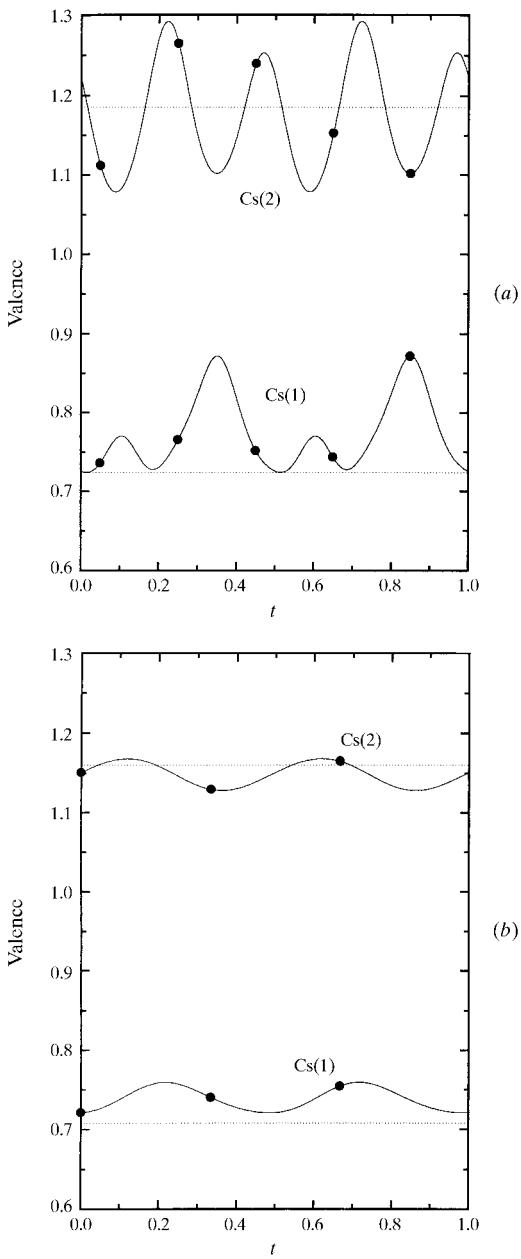


Fig. 6. Valences of Cs(1) and Cs(2) as a function of the fourth superspace coordinate. (*a*) The 5*a* superstructure {basic structure $V$[Cs(1)] = 0.72, $V$[Cs(2)] = 1.18, modulated structure $V$[Cs(1)] = 0.77, $V$[Cs(2)] = 1.17}; (*b*) the 3*c* superstructure {basic structure $V$[Cs(1)] = 0.71, $V$[Cs(2)] = 1.16, modulated structure $V$[Cs(1)] = 0.74, $V$[Cs(2)] = 1.15}. The dotted lines represent the values in the basic structures. Valences are calculated by the bond-valence method with $R^0$(Cs—Cl) = 2.791 Å (Brese & O'Keeffe, 1991).

For the commensurate modulations the true structure is obtained by one particular section $t$ of superspace only. We have determined these sections for both superstructures (Table 1). It is found that the 5*a* superstructure has a non-centrosymmetric space group for the supercell, while the 3*c* superstructure is centrosymmetric in three-dimensional space. These results are in accordance with the physical properties, which have indicated a polar symmetry for the 5*a* phase and a non-polar symmetry for the 3*c* phase (Dmitriev *et al.*, 1988; Kallayev *et al.*, 1990).

It is likely that the symmetries of the other modulated phases are described by the same superspace groups as presently determined for the 5*a* and 3*c* modulated structures. For the incommensurately modulated structures, the superspace group gives the complete symmetry, and these phases will show the behaviour according to a centrosymmetric symmetry. For the commensurate modulations, the appropriate section $t$ of superspace needs to be determined in each case. The supercell space group can then be obtained from Table 2. It is noted that dependent on $t$, either a centrosymmetric or non-centrosymmetric supercell space group is obtained.

We thank Dr Yu. Yuzyuk for providing the crystals and Dr W. Morgenroth for assistance with the synchrotron experiment. Financial support was obtained from the Deutsche Forschungsgemeinschaft DFG (German Science Foundation) and the Fonds der chemischen Industrie.

## References

Aalst, W. van, Hollander, J. den, Peterse, W. J. A. M. & De Wolff, P. M. (1976). *Acta Cryst.* B**32**, 47–58.

Bagautdinov, B. & Brown, I. D. (1997). Unpublished.

Bagautdinov, B., Luedecke, J., Schneider, M. & van Smaalen, S. (1998). *Acta Cryst.* B**54**, 626–634.

Becker, P. J. & Coppens, P. (1974). *Acta Cryst.* A**30**, 129–147.

Boguslavskii, A. A., Lotfullin, R. S., Simonov, M. V., Kirilenko, V. V., Pakhomov, V. I. & Mikhailova, A. Y. (1985). *Sov. Phys. Solid State*, **27**, 321.

Brese, N. & O'Keeffe, M. (1991). *Acta Cryst.* B**47**, 192–197.

Brown, I. D. (1992). *Acta Cryst.* B**48**, 553–572.

Cummins, H. Z. (1990). *Phys. Rep.* **185**, 211–409.

Dmitriev, V. P., Yuzyuk, Y. I., Tregubchenko, A. V., Larin, E. S., Kirilenko, V. V. & Pakhomov, V. I. (1988). *Sov. Phys. Solid State*, **30**, 704–705.

Fabry, J. & Perez-Mato, J. M. (1994). *Phase Transit.* **49**, 193–229.

Iizumi, M., Axe, J. D., Shirane, G. & Shimaoka, K. (1977). *Phys. Rev. B*, **15**, 4392–4411.

Janssen, T. (1986). *Ferroelectrics*, **66**, 203–216.
Kallayev, S. N., Gladkii, V. V., Kirikov, V. A. & Kamilov, I. K. (1990). *Ferroelectrics*, **106**, 299–302.
Linde, S. A., Mikhailova, A. Y., Pakhomov, V. I., Kirilenko, V. V. & Shulga, V. G. (1983). *Koord. Khim.* **9**, 998–999.
Madariaga, G., Alberdi, M. M. & Zuniga, F. J. (1990). *Acta Cryst.* C**46**, 2363–2366.
Madariaga, G., Zuniga, F. J., Paciorek, W. A. & Bocanegra, E. H. (1990). *Acta Cryst.* B**46**, 620–628.
Petricek, V. & Dusek, M. (1998). *JANA*98. Institute of Physics, Academy of Sciences, Praha, Czech Republic.
Sheldrick, G. M. (1996). *SADABS*. *Siemens Area Detector Absorption Correction Software*. University of Göttingen, Germany.
Siemens (1996). *SAINT*. *Area Detector and Integration Software*. Siemens Analytical X-ray Instruments Inc., Madison, Wisconsin, USA.
Smaalen, S. van (1987). *Acta Cryst.* A**43**, 202–207.
Smaalen, S. van (1995). *Crystallogr. Rev.* **4**, 79–202.
Werk, M. L., Chapuis, G. & Zuniga, F. J. (1990). *Acta Cryst.* B**46**, 187–192.
Wolff, P. M. de, Janssen, T. & Janner, A. (1981). *Acta Cryst.* A**37**, 625–636.